First Measurement of the Gerasimov-Drell-Hearn Sum Rule for ¹H from 0.7 to 1.8 GeV at ELSA

H. Dutz,[1] K. Helbing,[2] J. Krimmer,[3] T. Speckner,[2,*] G. Zeitler,[2,†] J. Ahrens,[4] S. Altieri,[5] J. R. M. Annand,[6] G. Anton,[2] H.-J. Arends,[4] R. Beck,[4] A. Bock,[2] C. Bradtke,[7] A. Braghieri,[5] W. v. Drachenfels,[1] F. Frommberger,[1] M. Godo,[2] S. Goertz,[7] P. Grabmayr,[3] S. Hasegawa,[8] K. Hansen,[9] J. Harmsen,[7] E. Heid,[4] W. Hillert,[1] H. Holvoet,[10] N. Horikawa,[11] T. Iwata,[8] L. Van Hoorebeke,[10] N. d'Hose,[12] P. Jennewein,[4] B. Kiel,[2] F. Klein,[1] R. Kondratiev,[13] M. Lang,[4] B. Lannoy,[10] R. Leukel,[4] V. Lisin,[13] D. Menze,[1] W. Meyer,[7] T. Michel,[2] J. Naumann,[2] A. Panzeri,[5] P. Pedroni,[5] T. Pinelli,[5] I. Preobrajenski,[4] E. Radtke,[7] G. Reicherz,[7] C. Rohlof,[1] T. Rostomyan,[10] M. Sauer,[3] B. Schoch,[1] M. Schumacher,[14] G. Tamas,[12] A. Thomas,[4] R. van de Vyver,[10] W. Weihofen,[14] and F. Zapadtka[14]

(GDH Collaboration)

[1]*Physikalisches Institut, Universität Bonn, D-53115 Bonn, Germany*
[2]*Physikalisches Institut, Universität Erlangen-Nürnberg, D-9l058 Erlangen, Germany*
[3]*Physikalisches Institut, Universität Tübingen, D-72076 Tübingen, Germany*
[4]*Institut für Kernphysik, Universität Mainz, D-55099 Mainz, Germany*
[5]*INFN, Sezione di Pavia, I-27100 Pavia, Italy*
[6]*Department of Physics and Astronomy, University of Glasgow, Glasgow G12 8QQ, United Kingdom*
[7]*Institut für Experimentalphysik, Ruhr-Universität Bochum, D-44801 Bochum, Germany*
[8]*Department of Physics, Nagoya University, Chikusa-ku, Nagoya, Japan*
[9]*MAX-lab, University of Lund, Box 118, S-221 00 Lund, Sweden*
[10]*Subatomaire en Stralingsfysica, Universiteit Gent, B-9000 Gent, Belgium*
[11]*CIRSE, Nagoya University, Chikusa-ku, Nagoya, Japan*
[12]*CEA Saclay, DSM/DAPNIA/SPhN, F-9ll9l Gif-sur-Yvette CEDEX, France*
[13]*INR, Academy of Science, Moscow, Russia*
[14]*II. Physikalisches Institut, Universität Göttingen, D-37073 Göttingen, Germany*

To verify the fundamental Gerasimov-Drell-Hearn (GDH) sum rule for the first time experimentally, we measured the helicity dependent total photoabsorption cross section with circularly polarized real photons and longitudinally polarized nucleons in the photon energy range 0.68–1.82 GeV with the tagged photon facility at ELSA. The experiment was carried out with a 4π detection system, a circularly polarized tagged photon beam, and a frozen spin polarized proton target. The contribution to the GDH sum rule in this photon energy range is $[49.9 \pm 2.4(\text{stat}) \pm 2.2(\text{syst})]$ μb.

I. Introduction.—The Gerasimov-Drell-Hearn (GDH) sum rule was derived in the mid-1960s by several authors. Gerasimov [1] and Drell and Hearn [2] used the framework of dispersion theory while the derivation by Hosada and Yamamoto [3] relied on the current algebra formalism. The sum rule connects well-known static properties of the nucleon, such as the anomalous magnetic moment κ_N and the mass m to its dynamic observables, i.e., the total cross section σ for the absorption of circularly polarized real photons on longitudinally polarized nucleons in the helicity states $3/2$ (spins parallel) and $1/2$ (spins antiparallel). Its difference is weighted by the inverse of the photon energy, ν, and integrated up to infinity:

$$\int_0^\infty [\sigma_{3/2}(\nu) - \sigma_{1/2}(\nu)] \frac{d\nu}{\nu} = \frac{2\pi^2 \alpha}{m^2} \kappa_N^2 [= 205 \ \mu\text{b} \ (^1\text{H})], \tag{1}$$

where α denotes the fine-structure constant. The dispersion theoretical derivation of the sum rule is based on very

fundamental physical principles: Lorentz and gauge invariance allow the Compton forward amplitude to be expressed in a general form. Unitarity leads to the optical theorem; due to causality the Compton forward amplitude is analytic. Under the assumption that *no subtraction* is necessary, a contour integration leads to a dispersion relation. The low theorem [4,5] is based again on Lorentz and gauge invariance and connects the spin-dependent scattering amplitude in first order of photon energy with κ_N and m and in third order with the spin polarizability, γ_0. A comparison of the first and third order terms, respectively, with the Taylor expanded dispersion relation gives the GDH sum rule [Eq. (1)] and an expression for the forward spin polarizability, γ_0, respectively:

$$-\frac{1}{4\pi^2} \int_0^\infty [\sigma_{3/2}(\nu) - \sigma_{1/2}(\nu)] \frac{d\nu}{\nu^3} = \gamma_0. \tag{2}$$

The experimental verification of the sum rule represents a validation of the above mentioned fundamental

principles and, most crucially, of the *no-subtraction hypothesis*. Furthermore, the energy dependence of the cross section in the two helicity states gives important constraints for multipole analyses in the resonance region, on the one hand, and makes restrictions about the validity of Regge models, on the other hand.

The GDH experiment is carried out at two accelerators to cover a wide photon energy range. At MAMI (Mainz), we measured the low energy part of the resonance region from 0.2 to 0.8 GeV [6–8]. With the experimental setup at the electron stretcher accelerator, ELSA (Bonn), we cover the photon energy range from 0.68 to 2.9 GeV. In the present Letter, we present the helicity dependence of the total photoabsorption cross section on the proton in the photon energy range from 0.68 to 1.82 GeV.

II. Experimental setup at ELSA. —The primary aim of the experimental conception was to measure the total photoabsorption cross section difference $\Delta\sigma(\nu) = \sigma_{3/2}(\nu) - \sigma_{1/2}(\nu)$ as a function of the photon energy, ν, with a minimal systematic error.

The polarization of the electrons delivered by ELSA was typically 70% at a maximum extracted beam current of 2 nA [9,10] and was permanently measured by the GDH-Møller polarimeter [11–13]. Circularly polarized photons, with polarization $P_{circ}(\nu, E_0)$, were produced by bremsstrahlung from longitudinally polarized electrons in a thin metal radiator foil (Cu 15 μm) via the helicity transfer [14]. The tagging system [15] covers an energy range of $(68\%–97\%) \times E_o$. Three primary electron energy settings (1.0, 1.4, and 1.9 GeV) were necessary to cover the photon energy range from 0.68 to 1.82 GeV. Active collimators [16] in the photon beam line are necessary to eliminate low energy photon background produced by the collimation process and to correctly determine the photon flux. To fulfill both purposes, the signal of the active collimators was used as a veto. The photon definition probability, $P_\gamma(\nu)$, relates the electron flux, $\Phi_{Tag}(\nu)$ to the photon flux in the tagged energy range at the hadronic target, $\Phi_\gamma(\nu) = P_\gamma(\nu)\Phi_{Tag}(\nu)$. The quantity $P_\gamma(\nu)$ was continuously measured with a total absorbing lead glass detector and the active collimators [17]. Typical values were of the order of 40% at 1.0 GeV, 55% at 1.4 GeV, and 70% at 1.9 GeV with a systematic uncertainty between 1.7% and 0.6%. A photon camera [18] was used to monitor the photon beam position.

The actively collimated photon beam impinged on the longitudinally polarized frozen spin butanol [H(CH$_2$)$_4$OH] target which was contained within a horizontal ^{3}He/^{4}He dilution cryostat [19]. The H nuclei were polarized typically up to 80% with relaxation times of up to 200 h. The target polarization, P_t, was measured by an NMR system with a precision of 1.1% to 2.8%. The target density of $f_t = 1.40 \times 10^{23}$ hydrogen nuclei per cm^2 was known with a systematic uncertainty of 2.3% [20].

In the ELSA photon energy range, photoabsorption processes lead to multiparticle final states which are hard to detect all individually with full acceptance and efficiency. To avoid systematic uncertainties arising from unobserved final states, the total photoabsorption cross section was measured inclusively. The concept of the GDH detector [21] is to observe at least one reaction product of all possible hadronic final states with almost complete acceptance as far as solid angle and efficiency are concerned. The detector is supplemented in the forward direction by the STAR detector [22]. The detection efficiency for the hadronic final states is higher than 99% and the solid angle coverage is 99.6% of 4π. With the help of a threshold CO_2-Čerenkov detector in forward direction, electromagnetic background events can be detected and suppressed with an efficiency of $(99.990 \pm 0.003)\%$.

Veto dead time effects occur due to random coincidences between the tagging system and the vetos (CO_2-Čerenkov detector, lead glass detector, active collimators). This veto dead time was measured precisely with a systematic uncertainty of $\pm0.6\%$ [23] and was used to correct for the hadronic count rate.

The complete setup has been tested extensively with unpolarized beam and solid state targets such as Be, C, and [CH$_2$]$_n$. The results are in excellent agreement with literature data and present an improvement with respect to statistical and systematical precision [17,23–25]. This shows the reliability of the whole setup and of the analysis procedure. In addition, we performed test measurements with polarized beam and/or polarized target to investigate possible sources of fake asymmetries. All results are compatible with zero [17].

III. Data analysis and systematic errors. —The energy and helicity dependent cross section difference $\Delta\sigma(\nu)$ is obtained by

$$\sigma_{3/2}(\nu) - \sigma_{1/2}(\nu) = \frac{Y_{3/2}(\nu) - Y_{1/2}(\nu)}{P_\gamma(\nu)f_t P_t P_{circ}(\nu, E_o)}. \qquad (3)$$

The quantities $P_\gamma(\nu)$, f_t, P_t, and $P_{circ}(\nu, E_o)$ have already been discussed. The hadronic yield $Y_{3/2,1/2}(\nu)$ is determined by the hadronic count rate of the GDH detector in each helicity state and is normalized to the photon flux, $\Phi_{Tag}(\nu)$, measured by the tagging system. A hadronic event is identified by at least one particle detected in one of the 15 detection units of the GDH detector, provided it is time correlated with an associated event in the tagging system. To avoid double counting, events where more than one unit has identified a particle are counted with a corresponding weight. In principle, electromagnetic background events are suppressed by the veto detectors, only very low energy electrons and positrons below the Čerenkov threshold of 18.5 MeV are misleadingly counted as hadronic events. In the analysis, these background events can be suppressed by their random character and their lower energy deposition compared to

TABLE I. The different contributions δ to the total systematic error $\delta(\sigma_{3/2} - \sigma_{1/2})$ for three primary energies E_o.

Primary energy E_o	1.0 GeV	1.4 GeV	1.9 GeV
Hadronic yield:			
δ (QDC cuts)	$\pm 0.7\%$	$\pm 0.7\%$	$\pm 0.7\%$
δ (veto dead time)	$\pm 0.6\%$	$\pm 0.6\%$	$\pm 0.6\%$
δ (absorption)	$\pm 1.0\%$	$\pm 0.5\%$	0.0%
Target:			
$\delta(f_t)$	$\pm 2.3\%$	$\pm 2.3\%$	$\pm 2.3\%$
$\delta(P_t)$	$\pm 2.8\%$	$\pm 2.8\%$	$\pm 1.1\%$
Photons:			
$\delta(P_\gamma)$	$\pm 1.7\%$	$\pm 0.6\%$	$\pm 1.2\%$
$\delta(P_{\text{circ}})$	$\pm 2.0\%$	$\pm 2.0\%$	$\pm 2.1\%$
Total $\delta(\sigma_{3/2} - \sigma_{1/2})$	$\pm 4.7\%$	$\pm 4.3\%$	$\pm 3.6\%$

FIG. 1. Doubly polarized total cross section difference for the proton compared to model calculations. Only statistical errors are shown.

hadronic events. The application of a minimum energy threshold [charge-to-digital-converter (QDC) cut] reduces their effect on the statistical error. Since only untagged photons can produce background events which are completely uncorrelated (random) with the tagging system, they can be subtracted from the time-correlated (prompt) events. A prerequisite for such a procedure is the observed negligible fraction of less than 10^{-3} of events which occurred as prompt in one module and as random in another one.

Regarding the cross sections, the values of the energy cuts (QDC cuts) tolerable at maximum were determined by varying them in the analysis of both doubly polarized and unpolarized data which we took periodically. As a result, the energy cuts were chosen such that within an error of 0.7% no changes in the cross sections were observed. The systematic uncertainty for $\Delta Y(\nu)$ which is caused by absorption effects in the target material and components of the cryostat — especially for single-pion production — falls strongly with increasing energy. The contributions to the systematic error with respect to $\Delta\sigma(\nu)$ are summarized in Table I. The total systematic error is obtained by summing all contributions in quadrature.

It should be stressed that the GDH setup at ELSA is able to measure total cross sections inclusively without the need for any extrapolation techniques due to almost full acceptance concerning solid angle and efficiency.

IV. Results and Discussion.—Figure 1 shows our results for the doubly polarized total cross section difference for the proton measured at ELSA at primary electron energies of 1.0, 1.4, and 1.9 GeV. The data are plotted together with the already published MAMI results [7]. The data sets from the different accelerators and from various primary electron energy settings overlap and match very well. The second [$D_{13}(1520)$] and third [$F_{15}(1680)$] resonances are clearly visible. The measured difference is positive up to 1.8 GeV and shows a structure in the "fourth resonance" region, which may indicate that the $F_{35}(1905)$
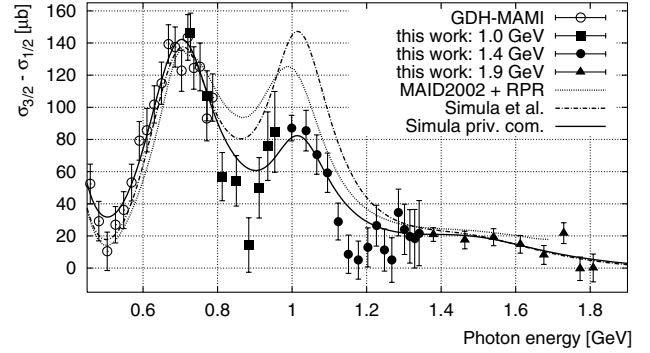
and $F_{37}(1950)$ resonances contribute significantly. Our data is also compared to theoretical models: The unitary isobar model MAID [26,27] in the "2002" solution [28] — a combination of the single-π and η parametrization [29] — fits together with the Reggeized $\pi\pi$ prediction from the Regge-plus-resonances (RPR) model [30,31] reasonably in the second resonance but overestimates $\Delta\sigma$ in the dip region between the second and the third resonances. Simula *et al.* [32] performed a Regge-based fit to deep inelastic scattering data and extrapolated to $Q^2 = 0$. As in the MAID2002 model [28], they took into account the main four-star resonances up to $W = 2$ GeV—$P_{33}(1232)$, $P_{11}(1440)$, $D_{13}(1520)$, $S_{11}(1535)$, $S_{11}^{\star}(1650)$, $D_{15}(1675)$, $F_{15}(1680)$, $D_{33}(1700)$, $F_{35}(1905)$, $F_{37}(1950)$— but simply added them incoherently to the Regge background. Figure 1 shows also a modified version where the width of the P_{33} as well as the strengths and the widths of the D_{13} and F_{15} resonances were adjusted to our data [33].

The helicity dependent cross sections $\sigma_{3/2}$ and $\sigma_{1/2}$ can be determined separately by means of the known unpolarized cross section for hydrogen $\sigma_{\text{tot}} = \frac{1}{2}(\sigma_{3/2} + \sigma_{1/2})$
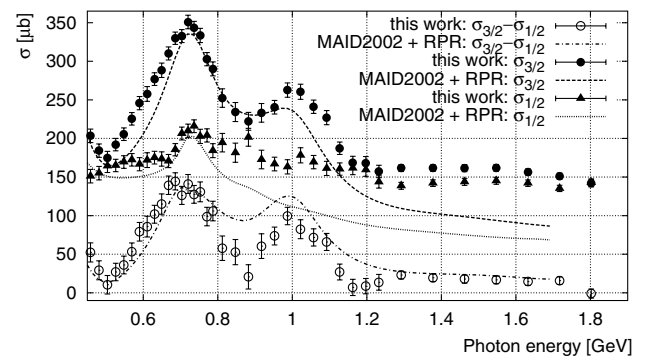

FIG. 2. Helicity dependent cross sections $\sigma_{3/2}$ and $\sigma_{1/2}$ off the proton above the Δ resonance compared to the results of the MAID2002 and the RPR model. The data of the different energy settings are combined and appropriately rebinned. Only statistical errors are shown.
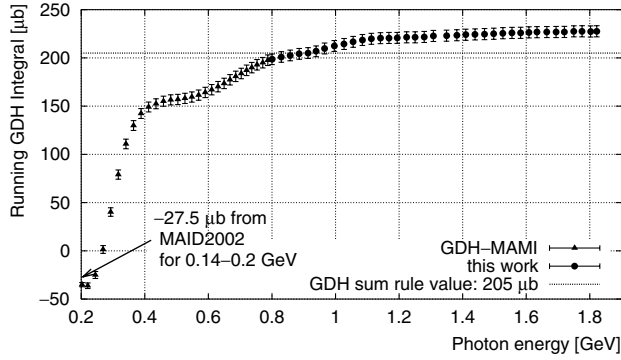
FIG. 3. Running GDH integral $I_{GDH} = \int_{\nu_0}^{E_\gamma} \Delta\sigma(\nu)\frac{d\nu}{\nu}$ up to $E_\gamma = 1.82$ GeV. Error bars indicate statistical errors only.

[34,35] and the measured difference $\Delta\sigma$: $\sigma_{3/2} = \sigma_{tot} + \frac{1}{2}\Delta\sigma$; $\sigma_{1/2} = \sigma_{tot} - \frac{1}{2}\Delta\sigma$. Figure 2 shows the results for the doubly polarized total cross sections $\sigma_{3/2}$ and $\sigma_{1/2}$ for the proton compared to the combined prediction of the MAID2002 and the RPR model. Missing contributions above a photon energy of 1 GeV may result from multiparticle final states not included in MAID and RPR.

In Fig. 3, we used the measured data to calculate the GDH integral, I_{GDH}, above the pion production threshold, ν_0, as a function of the upper integration limit. This so-called running GDH integral clearly overshoots the sum rule value for the proton of 205 μb, showing that the question of a sign change of $\Delta\sigma$ at higher energies is of prime importance. Purely electromagnetic contributions to κ_N — which can be nonvanishing below ν_0 — are of the order of $(\kappa_{e^-}/\kappa_N)^2 \sim 10^{-6}$ and are therefore neglected within this discussion. The measured value of I_{GDH} is shown in various photon energy intervals together with the γ_0 integral, I_{γ_0}, in Table II. I_{GDH} amounts to $[49.9 \pm 2.4(stat) \pm 2.2(syst)]$ μb between 0.68 and 1.82 GeV. Because of the ν^{-3} weighting, the contribution to I_{γ_0} in the energy range of 0.68–1.82 GeV is small and amounts to $[-6.6 \pm 0.3(stat) \pm 0.3(syst)] \times 10^{-6}$ fm^4.

Together with the previously measured data at MAMI [7], the photon energy interval covered experimentally is now much broader; however, it is still too narrow to draw any definitive conclusion about the validity of the GDH sum rule. A reasonable estimate of its value can be deduced by using the contributions predicted by existing models for the missing energy range: The unitary isobar

model MAID2002 gives a contribution of (-27.5 ± 3) μb for photon energies below 0.20 GeV [28] which we used as offset in Fig. 3. This gives a value for I_{GDH} between 0.14 and 1.82 GeV of 228 μb. We used Regge approaches from [33,36] and predict a negative contribution above 1.82 GeV of -22 μb [36] and -13 μb [33], respectively. The combination of our combined experimental results from MAMI and ELSA with these predictions yields an estimate (206–215 μb) which — within the experimental errors — is consistent with the GDH sum rule value [Eq. (1)]. Our measurements up to 2.9 GeV at ELSA will finally clarify the validity of Regge predictions [32,33,36] in this energy regime and will give a more definitive answer to the question whether the GDH sum rule holds or not.

Concerning I_{γ_0}, the unmeasured contribution from photon energies below 0.20 GeV is very important. MAID2002 predicts 90×10^{-6} fm^4 [28]. A combination with our experimental results from MAMI and ELSA (cf. Table II) gives a very good estimate of -100×10^{-6} fm^4 for γ_0 since within the energy of 1.8 GeV I_{γ_0} seems to be saturated due to the ν^{-3} weighting. A comparison of theoretical predictions for γ_0 can be found in Ref. [7].

---

*Author to whom correspondence may be addressed.
Electronic address: Thorsten.Speckner@physik.uni-erlangen.de
†Author to whom correspondence may be addressed.
Electronic address: Guenter.Zeitler@physik.uni-erlangen.de

[1] S. B. Gerasimov, Sov. J. Nucl. Phys. **2**, 430 (1966).
[2] S. D. Drell and A. C. Hearn, Phys. Rev. Lett. **16**, 908 (1966).
[3] M. Hosada and K. Yamamoto, Prog. Theor. Phys. **36**, 425 (1966).
[4] F. E. Low, Phys. Rev. **96**, 1428 (1954).
[5] M. Gell-Mann and M. L. Goldberger, Phys. Rev. **96**, 1433 (1954).
[6] J. Ahrens et al., Phys. Rev. Lett. **84**, 5950 (2000).
[7] J. Ahrens et al., Phys. Rev. Lett. **87**, 022003 (2001).
[8] J. Ahrens et al., Phys. Rev. Lett. **88**, 232002 (2002).
[9] S. Nakamura et al., Nucl. Instrum. Methods Phys. Res., Sect. A **411**, 93 (1998).
[10] M. Hoffmann et al., AIP Conf. Proc. **570**, 756 (2001).
[11] B. Kiel, Ph.D. thesis, University Erlangen, 1999.
[12] T. Speckner, Ph.D. thesis, University Erlangen, 2002.
[13] T. Speckner et al., Nucl. Instrum. Methods Phys. Res., Sect. A (to be published).
[14] H. Olsen and L. C. Maximon, Phys. Rev. **114**, 887 (1959).

TABLE II. Measured values of the GDH integral, I_{GDH}, and the γ_0 integral, I_{γ_0}, in various photon energy intervals.

	E_γ [GeV]	I_{GDH} [μb]	I_{γ_0} [10^{-6} fm^4]
ELSA	0.68–1.82	$49.9 \pm 2.4 \pm 2.2$	$-6.6 \pm 0.3 \pm 0.3$
ELSA	0.80–1.82	$29.1 \pm 1.9 \pm 1.3$	$-2.7 \pm 0.2 \pm 0.1$
MAMI-B [7]	0.20–0.80	$226 \pm 5 \pm 12$	$-187 \pm 8 \pm 10$
	0.20–1.82	$255 \pm 5 \pm 12$	$-190 \pm 8 \pm 10$

[15] J. Naumann *et al.*, Nucl. Instrum. Methods Phys. Res., Sect. A **498**, 211 (2003).

[16] G. Zeitler *et al.*, Nucl. Instrum. Methods Phys. Res., Sect. A **459**, 6 (2001).

[17] G. Zeitler, Ph.D. thesis, University Erlangen, 2002.

[18] J. Krimmer *et al.*, Nucl. Instrum. Methods Phys. Res., Sect. A **481**, 57 (2002).

[19] C. Bradtke *et al.*, Nucl. Instrum. Methods Phys. Res., Sect. A **436**, 430 (1999).

[20] C. Rohlof, Ph.D. thesis, University Bonn, 2003.

[21] K. Helbing *et al.*, Nucl. Instrum. Methods Phys. Res., Sect. A **484**, 129 (2002).

[22] M. Sauer *et al.*, Nucl. Inst. Meth. A **378**, 143 (1996).

[23] T. Michel, Ph.D. thesis, University Erlangen, 2001.

[24] T. Michel *et al.* (to be published).

[25] K. Helbing *et al.* (to be published).

[26] D. Drechsel *et al.*, Nucl. Phys. A **645**, 145 (1999).

[27] D. Drechsel *et al.*, Phys. Rev. D **63**, 114010 (2001).

[28] L. Tiator, Proceedings of GDH2002 (World Scientific, Singapore, 2003); (private communication).

[29] W.-T. Chiang *et al.*, Nucl. Phys. A **700**, 429 (2002).

[30] H. Holvoet, Ph.D. thesis, University Gent, 2001.

[31] H. Holvoet and M. Vanderhaeghen (to be published).

[32] S. Simula *et al.*, Phys. Rev. D **65**, 034017 (2002).

[33] S. Simula (private communication).

[34] Particle Data Group, D. E. Groom *et al.*, Eur. Phys. J. C **15**, 1 (2000).

[35] M. MacCormick *et al.*, Phys. Rev. C **53**, 41 (1996).

[36] N. Bianchi and E. Thomas, Phys. Lett. B **450**, 439 (1999).